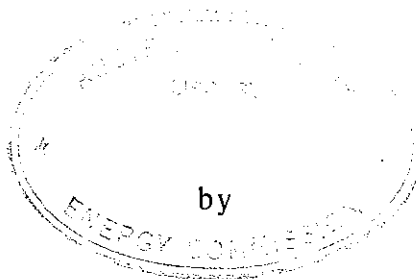




AUSTRALIAN ATOMIC ENERGY COMMISSION  
RESEARCH ESTABLISHMENT  
LUCAS HEIGHTS

A WORK-HARDENING CORRECTION FOR STRESS RELAXATION  
DERIVED CREEP PROPERTIES



J.T.A. POLLOCK  
R. CLISSOLD

June 1981

ISBN 0 642 59714 6



AUSTRALIAN ATOMIC ENERGY COMMISSION  
RESEARCH ESTABLISHMENT  
LUCAS HEIGHTS

A WORK-HARDENING CORRECTION FOR STRESS RELAXATION  
DERIVED CREEP PROPERTIES

by

J.T.A. POLLOCK  
R. CLISSOLD

ABSTRACT

A work-hardening correction has been added to a previously devised method for characterising the long-term deformation properties of metals and alloys by derivation from short-term relaxation data. The usefulness of this correction has been assessed by creep and stress relaxation measurements on titanium, copper and 70/30 brass. Within defined strain limits, good agreement is obtained between derived and directly measured creep parameters. The importance of the relaxation-system spring constant in determining the extent of the agreement is discussed.

National Library of Australia card number and ISBN 0 642 59714 6

The following descriptors have been selected from the INIS Thesaurus to describe the subject content of this report for information retrieval purposes. For further details please refer to IAEA-INIS-12 (INIS: Manual for Indexing) and IAEA-INIS-13 (INIS: Thesaurus) published in Vienna by the International Atomic Energy Agency.

STRAIN HARDENING; STRESS RELAXATION; CREEP; TITANIUM; COPPER; BRASS; GAS CENTRIFUGES; MEDIUM TEMPERATURE; CORRECTIONS; DEFORMATION

## CONTENTS

|  |    |
|--|----|
| 1. INTRODUCTION  | 1  |
| 2. EXPERIMENTAL PROCEDURES   | 1  |
| 2.1 Stress Relaxation and Creep Measurements   | 2  |
| 3. DERIVATION OF CONSTANT LOAD CREEP DATA FROM STRESS RELAXATION DATA  | 2  |
| 4. RESULTS   | 4  |
| 4.1 Titanium   | 4  |
| 4.2 70/30 Brass  | 5  |
| 4.3 Commercial Copper  | 6  |
| 5. DISCUSSION  | 7  |
| 6. CONCLUSIONS   | 9  |
| 7. REFERENCES  | 10 |
| Figure 1 Tensile stress/strain data for materials investigated   | 11 |
| Figure 2 Titanium. Relaxed load versus log time  | 12 |
| Figure 3 Titanium. Creep strain versus log time  | 13 |
| Figure 4 Titanium. Directly measured and derived creep parameters ( $\lambda = 1.3 \times 10^4 \text{ N mm}^{-2}$ ) versus applied stress  | 14 |
| Figure 5 Titanium. Directly measured and derived creep parameters ( $\lambda = 1.3 \times 10^3 \text{ N mm}^{-2}$ ) versus applied stress  | 15 |
| Figure 6 70/30 brass. Relaxed load versus log time   | 16 |
| Figure 7 70/30 brass. Creep strain versus log time   | 17 |
| Figure 8 70/30 brass. Directly measured and derived creep parameters ( $\lambda = 8 \times 10^3 \text{ N mm}^{-2}$ ) versus applied stress | 18 |
| Figure 9 Copper. Relaxed load versus log time ( $\lambda = 9 \times 10^2 \text{ N mm}^{-2}$ )  | 19 |

|            |  |    |
|------------|--|----|
| Figure 10  | Copper. Relaxed load ( $\lambda = 9 \times 10^3 \text{ N mm}^{-2}$ ) versus log time   | 20 |
| Figure 11  | Copper. Creep strain versus log time   | 21 |
| Figure 12  | Copper. Directly measured and derived creep parameters ( $\lambda = 9 \times 10^2 \text{ N mm}^{-2}$ ) versus applied stress | 22 |
| Figure 13  | Copper. Directly measured and derived creep parameters ( $\lambda = 9 \times 10^3 \text{ N mm}^{-2}$ ) versus applied stress | 23 |
| Figure 14  | Titanium. Work hardening slope, $W$ , versus stress  | 24 |
| Figure 15  | Copper. Work hardening slope, $W$ , versus stress  | 24 |
| Figure 16  | Copper. Stress relaxation parameter, measured and derived, versus stress for various spring constants                        | 25 |
| Appendix A | Derivation of $\theta$ and $1 + \frac{\theta}{\lambda}$  | 27 |

## 1. INTRODUCTION

The ambient temperature, creep properties of very strong materials, like high strength steels, are reported in the literature. Most room temperature applications of such materials assume that plastic deformation does not occur up to 80 per cent ultimate tensile strength (UTS). Gas centrifuges for uranium enrichment are a critical application for which such information is mandatory. Since the direct measurement of creep properties can be time consuming, the AAEC has established a short-term method for characterising the long-term deformation properties of any steel or alloy by derivation from short-term stress relaxation data. Reports on the application of this method to maraging steels have been published [Pollock and Barton 1976, 1979]. The procedure is based on the method for correlating creep and stress relaxation data, outlined by Feltham [1961] which was uncorrected for work-hardening. Subsequently, Krausz and Craig [1966] examined Feltham's approach and highlighted the importance of relaxation machine stiffness in determining the agreement between the relaxation derived and the directly measured creep properties.

Pollock and Barton [1979] attempted to account for work-hardening during relaxation in their maraging steel work; however, the errors invoked in calculating the correction were large owing to the very high work-hardening rates of maraging steels. Although the agreement between derived and directly measured parameters was useful for design purposes, it was decided to examine the approach on more easily deformed materials. Also, the role of relaxation machine stiffness could be investigated.

The method has been applied to experimental creep and stress relaxation data measured with high purity titanium, commercial copper and 70/30 brass.

## 2. EXPERIMENTAL PROCEDURES

Round-shouldered tensile samples having gauge dimensions 20 mm long x 4 mm wide were stamped from thin sheets and used to determine the stress/strain relationships and stress relaxation characteristics. Round-shouldered tensile samples having gauge dimensions 100 mm x 2 mm wide were machined from the same sheets and used to determine creep properties.

## 2.1 Stress Relaxation and Creep Measurements

Stress relaxation measurements were carried out at  $35 \pm 0.25^\circ\text{C}$  and a constant loading strain rate of  $8 \times 10^{-5} \text{ s}^{-1}$ , according to procedures described by Pollock and Barton [1979]. Continuous loading stress/strain data were measured under the same conditions. Following Krausz and Craig [1966], springs were used to investigate the effect of the loading-train spring constant on the agreement between derived and measured creep data. In all cases, the relaxation-system spring constant was measured from the initial elastic-loading record of the sample and, in many cases, checked by measuring on reloading after a series of relaxations.

Creep data were measured directly using high sensitivity, differential displacement rigs and procedures [Pollock and Barton 1979].

## 3. DERIVATION OF CONSTANT LOAD CREEP DATA FROM STRESS RELAXATION DATA

Feltham [1961] outlined a method for extracting creep parameters from stress relaxation data. The approach may be applied when

- (a) the total strains during relaxation and creep are small, and
- (b) there is a linear relationship between the logarithm of time and relaxed stress, or creep strain.

Condition (a) is generally satisfied with strong materials but, depending on the applied stress, it may not always be satisfied with softer materials. The experimental data provide a check on the satisfaction of condition (b).

The deformation occurring during stress relaxation and creep may be characterised by parameters calculated from the experimental data. From the relaxation data

$$S_R = - d\sigma / d \log_e t \quad (1)$$

may be measured, where  $\sigma$  is the applied stress at time  $t$ . From the creep data

$$S_C = d\varepsilon / d \log_e t \quad (2)$$

may be measured, where  $\epsilon$  is the creep strain at time  $t$ . Feltham [1961] demonstrated that these parameters were proportionally related as follows

$$S_R = S_C \times \theta \quad (3)$$

where  $\theta$  is the work-hardening coefficient, defined as  $d\sigma/d\epsilon_p$  at the load of interest measured from an uninterrupted stress/plastic strain curve.

Feltham [1961] ignored work-hardening when verifying Equation (3) experimentally, using well-annealed brass over a small stress range. The stress drop during a relaxation experiment is caused by continuing plastic deformation of the sample which replaces some of the elastic deformation of the loading train, since the total deformation (elastic plus plastic) of the system remains constant. If significant work-hardening occurs, the stress drop recorded will be less than that calculated from Equations (1) and (3).

Following Sargeant [1965] a correction factor for work-hardening during relaxation may be introduced [Pollock and Barton 1979]; Equation (3) then takes the corrected form

$$S_R \times \left(1 + \frac{\theta'}{\lambda}\right) = S_C \times \theta \quad (4)$$

where  $\lambda$  is the relaxation-system spring constant defined as

$$\lambda = d\sigma/d\epsilon_e \quad (5)$$

where  $d\epsilon_e$  is the elastic strain accompanying an increase in stress,  $d\sigma$ , and  $\theta'$  is the work-hardening rate before relaxation from the load of interest. Both the factor  $\left(1 + \frac{\theta'}{\lambda}\right)$  and the work hardening rate,  $\theta$ , may be easily obtained from the experimental chart record as shown in Appendix A. Equation (4) then takes the form

$$S_R \times \frac{M'}{M'-W'} = S_C \times \frac{MW}{M-W} \times \frac{\dot{C}}{S} \times \frac{l_0}{a_0} \quad (6)$$

where

$M =$  elastic-loading slope measured from the chart record during uninterrupted loading ( $N \text{ mm}^{-1}$ ),

$M'$  = elastic loading slope measured from the chart record during loading before relaxation testing ( $N\ mm^{-1}$ ),

$W$  = work hardening slope measured at the load of interest during uninterrupted loading ( $N\ mm^{-1}$ ),

$W'$  = work hardening slope measured before relaxation from the load of interest ( $N\ mm^{-1}$ ),

$l_0$  and  $a_0$  = initial gauge length (mm) and mass section ( $mm^2$ ), respectively, and

$\dot{C}$  and  $\dot{S}$  = fixed chart and cross-head speeds, respectively ( $mm\ m^{-1}$ ).

Normally,  $M = M'$  and  $W = W'$ , therefore Equation (6) reduces to

$$S_R = S_C \times W \times \frac{\dot{C}}{\dot{S}} \times \frac{l_0}{a_0} \quad (7)$$

When different machine elastic constants are used to determine uninterrupted stress/strain and incremental relaxation data,  $M \neq M'$  and  $W \neq W'$ . Nevertheless, for these conditions  $\frac{MW}{M-W} = \frac{M'W'}{M'-W'}$  and Equation (6) may be used in the form

$$S_{R(W')} = S_C \times W' \times \frac{\dot{C}}{\dot{S}} \times \frac{l_0}{a_0} \quad (8)$$

In cases where the loading history determines the work-hardening at a given load, the assumptions on which the analysis rests begin to falter, and the amplifications leading to Equations (7) and (8) are not applicable. However, under these circumstances Equation (6) may be applied. This was the case with 70/30 brass which exhibits strain-ageing characteristics.

## 4. RESULTS

### 4.1 Titanium

Titanium samples were stamped or machined from 0.71 mm thick sheets of 6N pure material and annealed in vacuum at 850°C for 60 minutes. The tensile stress/strain curve for this starting material is shown in Figure 1.

Stress relaxation and creep data were measured by incrementally loading a number of samples. Relaxed load and creep strain are plotted against the logarithm of time in Figures 2 and 3 respectively. The scales chosen for these figures are convenient for condensed presentation and show the variation in behaviour with stress. The relaxation data in Figure 2 were measured with a spring constant of  $1.3 \times 10^4 \text{ N mm}^{-2}$ . Other relaxation measurements were made with a softer spring constant of  $1.3 \times 10^3 \text{ N mm}^{-2}$ .

Directly measured creep parameters,  $S_C$ , calculated from the slopes of creep strain versus the logarithm of time, are shown as a function of stress in Figures 4 and 5. After correcting the relaxation data for the small amount of machine relaxation occurring at loads up to 600 N, relaxation parameters,  $S_R$ , were measured from the slopes of the relaxed load versus the logarithm of time. Derived creep parameters were then calculated using Equations (3) and (7) or (8). Creep parameters, derived from the relaxation data measured with the high spring constant are included in Figure 4. Using Equation (7), which contains the correction for work-hardening during relaxation, excellent agreement is obtained with the directly measured data. Using Equation (3), which is uncorrected for work-hardening, significantly lower creep rates are derived at all stress levels, in agreement with the expectation that a smaller relaxation stress drop will be recorded when work-hardening occurs.

Creep parameters derived from the relaxation data measured with the smaller spring constant are plotted against stress in Figure 5. Using Equation (8), reasonable agreement is obtained at stresses above  $140 \text{ N mm}^{-2}$ . At lower stresses, the agreement is poor and, as will be discussed later (Section 5), related to problems of accuracy when measuring the work-hardening slope,  $W'$ .

#### 4.2 70/30 Brass

70/30 brass samples were stamped or machined from 0.64 mm thick sheets of rolled material and annealed at  $760^\circ\text{C}$  for 30 minutes in sealed tubes, taking the usual precautions to prevent de-zincification. The tensile stress/strain curve is shown in Figure 1. Discontinuous yielding, evidence of strain-ageing [Hall 1970], was observed at stresses above  $65 \text{ N mm}^{-2}$ . This strain-ageing was also noted during the incremental loading of stress relaxation samples. On reloading after recording a relaxation, upper and lower yield points were observed, the upper yield point load being higher than the previous stress relaxation load.

Examples of the relaxation and creep data are plotted against the logarithm of time in Figures 6 and 7, respectively. Deviations from linearity due to strain ageing occurred for times greater than 200 seconds. The  $S_C$  parameters calculated directly from creep data are shown versus stress in Figure 8. Derived creep parameters, calculated using relaxation data measured with a spring constant of  $8 \times 10^3 \text{ N mm}^{-2}$  and Equations (3), (6) and (7), are also shown in Figure 8. Equation (6) was used since strain-ageing effects during loading ensured that the work-hardening conditions immediately before relaxation were not identical with those at the same load during an uninterrupted stress/strain test. Equation (6) provided reasonable agreement with the directly measured data over the short stress range up to approximately  $65 \text{ N mm}^{-2}$ . Each equation produced derived creep parameters which displayed an anomalous change to lower creep as stress increased from about  $65$  to  $70 \text{ N mm}^{-2}$ . Above  $70 \text{ N mm}^{-2}$ , the expected increase in creep with increased stress was obtained. The directly measured creep parameters reveal that this anomaly is a change in the rate of increase of creep parameter with stress to a lower rate above  $60 \text{ N mm}^{-2}$ .

Using the softer spring constant of  $1.3 \times 10^3 \text{ N mm}^{-2}$ , the work-hardening slope  $W'$  could not be measured accurately enough at lower stresses to provide any measure of agreement with directly measured creep parameters. At higher stresses, a wide disparity was obtained between derived and directly measured data.

#### 4.3 Commercial Copper

Commercial copper samples were stamped or machined from 1.0 mm thick sheets and annealed at  $800^\circ\text{C}$  for 10 minutes. The tensile stress/strain curve is shown in Figure 1. Relaxed load versus the logarithm of time data, measured with spring constants of  $9 \times 10^2 \text{ N mm}^{-2}$  and  $9 \times 10^3 \text{ N mm}^{-2}$ , are shown in Figures 9 and 10 respectively.

As was expected, the data measured with the lower spring constant produce smaller values of  $S_R$ . Creep parameters calculated directly from the creep data (Figure 11), are shown versus stress in Figure 12. Also included in Figure 12 are creep parameters derived from the relaxation data measured with the spring constant of  $9 \times 10^2 \text{ N mm}^{-2}$ , using Equations (3) and (8).

Equation (8), which is corrected for work-hardening, produces derived  $S_C$  values which are in good agreement with those measured directly. In Figure

13, creep parameters derived from stress relaxation data measured with the stiffer spring constant of  $9 \times 10^3 \text{ N mm}^{-2}$  are compared with the directly determined creep data. Neither Equation (3), uncorrected for work-hardening, nor Equation (7), which contains the work-hardening correction, provide derived creep parameters that compare favourably with directly measured data. This variation in derived creep parameters with spring constant is the same as that reported by Krausz and Craig [1966].

## 5. DISCUSSION

The experimental results measured with titanium and copper demonstrate that the work-hardening correction incorporated in Equations (6) and (7) or (8) produces a significant improvement in the agreement between directly measured creep data and those derived from stress relaxation results. With titanium, the agreement is excellent when derived from relaxation data measured with the stiffer spring constant (Figure 4), compared with that measured with the softer spring constant (Figure 5). With copper, the situation is reversed. The softer system (Figure 12) produces a better agreement with directly measured data. The role of the spring constant in determining the error in the measurement of the work-hardening slope can be shown to control the results for titanium. The case for copper is less clear. Because of strain-ageing effects, the results for 70/30 brass are completely different and will be discussed separately.

The spring constant,  $\lambda$ , of the system used for the measurement of stress relaxation or uninterrupted stress/strain data, determines the accuracy with which the work-hardening slope,  $W$ , and the relaxation parameter,  $S_R$  can be determined. Equation (7) indicates that these are the two variables upon which the analysis rests. The load drop was always sufficient for an accurate determination of  $S_R$ . However,  $W$  proved to be much more sensitive to variation in spring constant. The extent of this sensitivity may be understood by reference to Figure 14 where  $W$  values for titanium are plotted as a function of stress for two spring constants. An accurate measurement of  $W$ , as a function of stress, was impossible at stresses below  $140 \text{ N mm}^{-2}$  with the softer spring constant. The derived creep data (Figure 5) highlight the error arising from this inaccurately measured  $W$ . Agreement with the directly measured creep data was only approached at stresses above  $140 \text{ N mm}^{-2}$ .

These results for titanium show that with materials exhibiting high work-hardening rates, a stiff spring constant is required to ensure an accurate determination of the work-hardening slope. As the work-hardening rate decreases, the need for a stiff spring constant lessens; hence the improvement in correlation at stresses above  $140 \text{ N mm}^{-2}$  with the softer spring constant system.

Similar plots of  $W$  versus stress for copper are produced in Figure 15. Although the stiffer machine produces a more useful variation in  $W$  at stresses up to  $100 \text{ N mm}^{-2}$ , the variation measured with the softer machine was sufficient for accurate determinations. Indeed, as the derived data show (Figures 12 and 13), a better correlation with the directly measured creep parameters is obtained with the softer spring constant. These results agree with those reported by Krausz and Craig [1966], who derived the basic logarithmic relationship between time and relaxed load by solving Mott's [1953] equation for thermally activated flow.

Their solution took the form

$$S_{R_{KC}} = \frac{d\sigma}{d \log_e t} \left(1 + \frac{\theta}{\lambda}\right) \quad (8)$$

From Equation (1),  $S_R = d\sigma/d \log_e t$   
therefore,

$$S_{R_{KC}} = S_R \left(1 + \frac{\theta}{\lambda}\right) \quad (9)$$

This is the same expression as that obtained for the corrected relaxation parameter on the right hand side of Equation (4). However, Krausz and Craig [1966] did not discuss the role of work-hardening during relaxation, preferring to interpret Equation (9) as an expression of the role of the spring constant  $\lambda$ . Thus, using well annealed, electrolytic, tough pitch copper, they carried out a series of relaxation tests with different spring constants producing a family of curves (Figure 16) which show that  $S_{R_{KC}}$  is proportional to stress and increases with spring constant  $\lambda$ . Agreeing with Feltham [1961] that creep strain at constant load is proportional to the logarithm of time (Equation (2)), they derived  $S_R$  values from directly measured  $S_C$  values using Equation (3). These values are also included in Figure 16 and show that there is reasonable agreement between the derived  $S_R$  values and the  $S_{R_{KC}}$  values directly measured with the softer machine

constants.

Using the directly measured creep data reported here,  $S_R$  values were calculated using Equation (3). These values are also included in Figure 16 and, given the expected differences in sample purity, they agree well with those of Krausz and Craig [1966]. Figure 16 implies that there is a spring constant effect for copper and that good agreement with directly measured creep data will be obtained only with stress relaxation data measured with machines having spring constants  $< 5 \times 10^3 \text{ N mm}^{-2}$ . The reason for this effect is not clear. Krausz and Craig [1966] do not discuss it, stating only that structural changes, the most likely explanation, were not responsible.

The results for 70/30 brass indicate that the application of Equation (4) is limited to deformation processes which can be reasonably described as resulting from thermally activated dislocation motion. This is not the case at stress levels above  $65 \text{ N mm}^{-2}$  with 70/30 brass, where strain-ageing effects are significant. Below  $65 \text{ N mm}^{-2}$ , strain-ageing effects are small and Equation (6) was successfully used to derive creep values from stress relaxation data measured with the stiffer spring system. Equation (6) accounts for the occurrence of different work-hardening rates at the same load, reached by an incremental loading path in stress relaxation, and by an uninterrupted loading path for the determination of  $\theta$ . Under these circumstances a good agreement has been produced between the derived and directly measured parameters (Figure 8).

## 6. CONCLUSIONS

(a) Creep and stress relaxation data may be related as follows:

$$S_R \left( 1 + \frac{\theta'}{\lambda} \right) = S_C \times \theta \quad (4)$$

where  $\left( 1 + \frac{\theta'}{\lambda} \right)$  is a term which corrects the stress relaxation parameter,  $S_R$ , for work-hardening.

(b) For the relationship to apply, the deformation process must be simply described as thermally activated dislocation motion and must allow the calculation of  $S_R$  and  $S_C$  from linear plots of the logarithm of time versus relaxed stress and creep strain respectively.

(c) The relaxation-system spring constant plays an important role in determining the accuracy with which the work-hardening correction may be calculated. With high work-hardening materials, a high spring constant is required. This was the case for titanium.

(d) The data measured with copper agreed with those previously reported by Krausz and Craig [1966]. An improved agreement between derived and directly measured creep parameters was found with softer relaxation spring systems, but these have yet to be satisfactorily explained.

## 7. REFERENCES

Feltham, P. [1961] - J. Inst. Met., 89:210.

Hall, E.O. [1970] - Yield Point Behaviour in Metals and Alloys, McWilliam, London.

Krausz, A.S. and Craig, G.B. [1966] - Acta Metall., 14:1807.

Mott, N.F., [1953] - Phil. Mag., 44:742.

Pollock, J.T.A. and Barton, S.G. [1976] - AAEC/E381.

Pollock, J.T.A. and Barton, S.G. [1979] - AAEC/E462.

Sargeant,, G.A. [1965] - Acta Metall., 13:603.

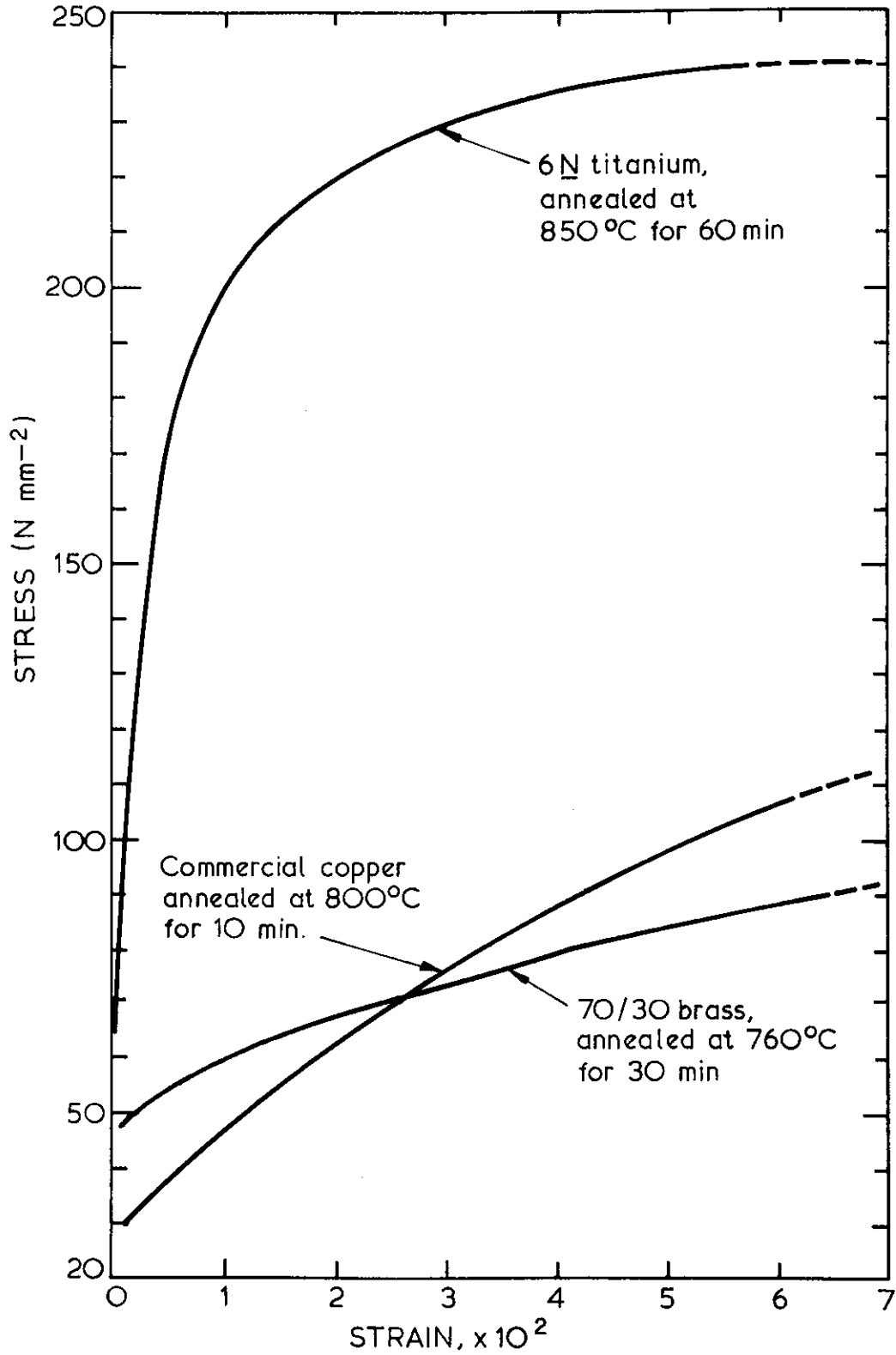


FIGURE 1. TENSILE STRESS/STRAIN DATA FOR MATERIALS INVESTIGATED

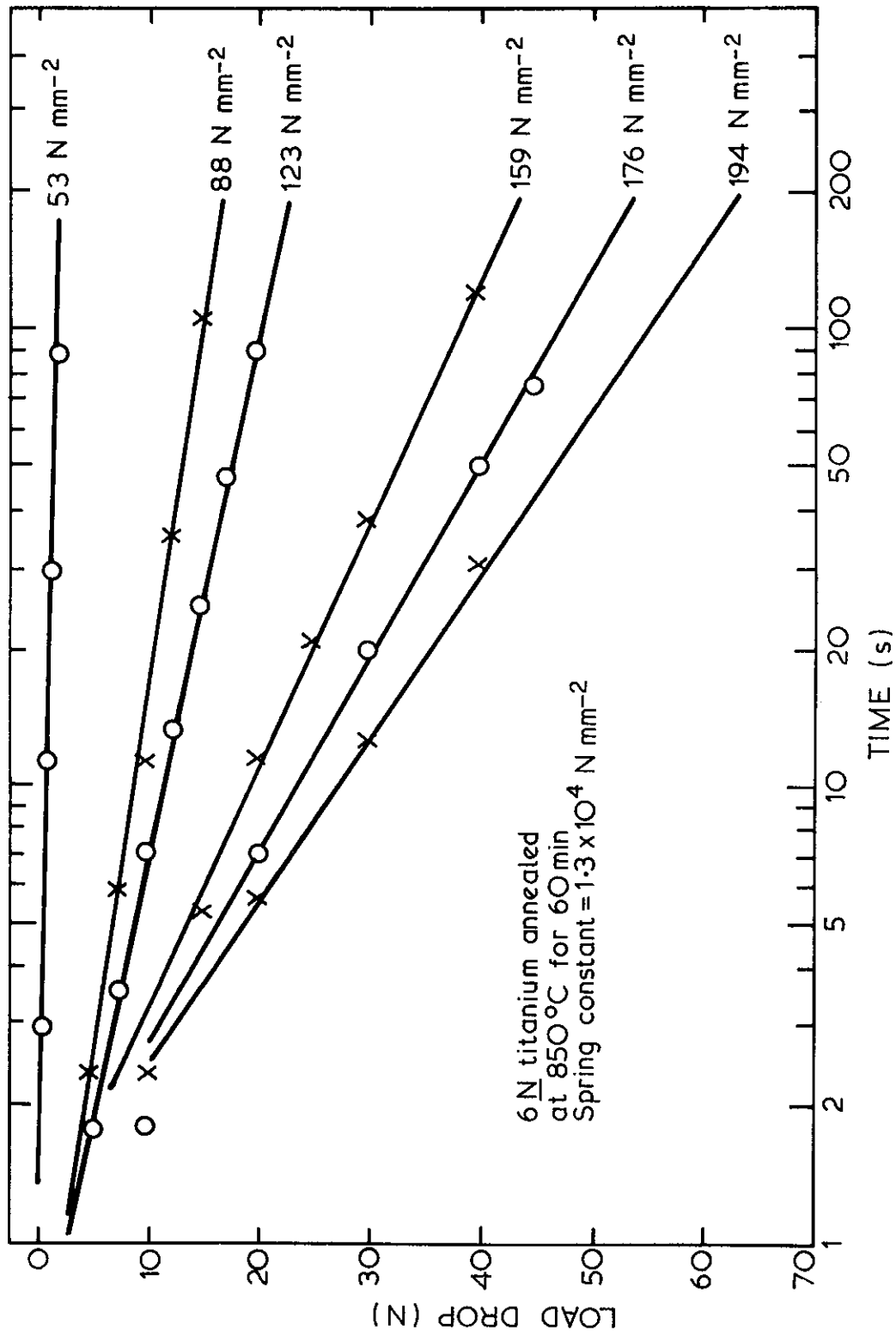


FIGURE 2. TITANIUM. RELAXED LOAD VERSUS LOG TIME

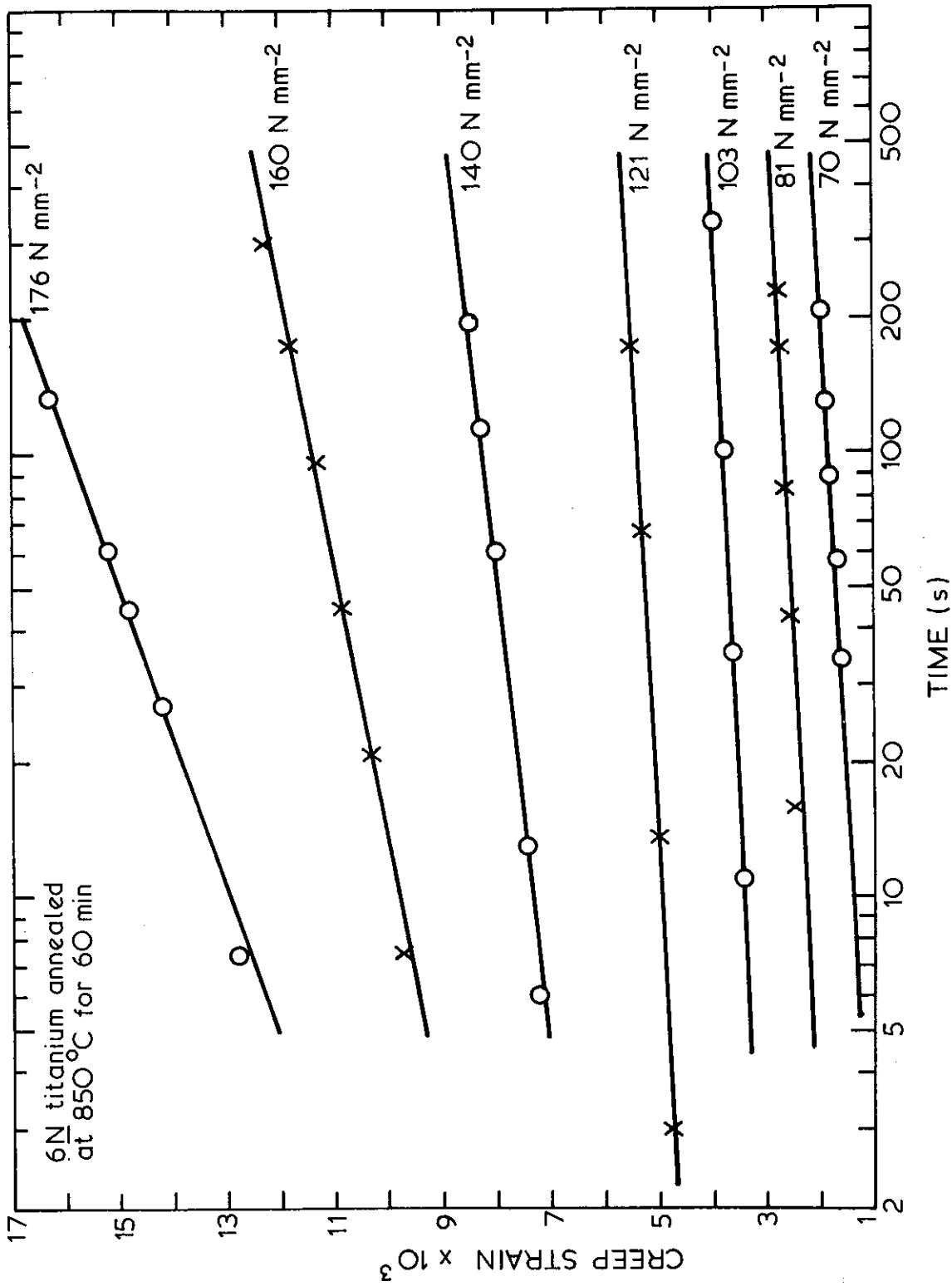


FIGURE 3. TITANIUM. CREEP STRAIN VERSUS LOG TIME

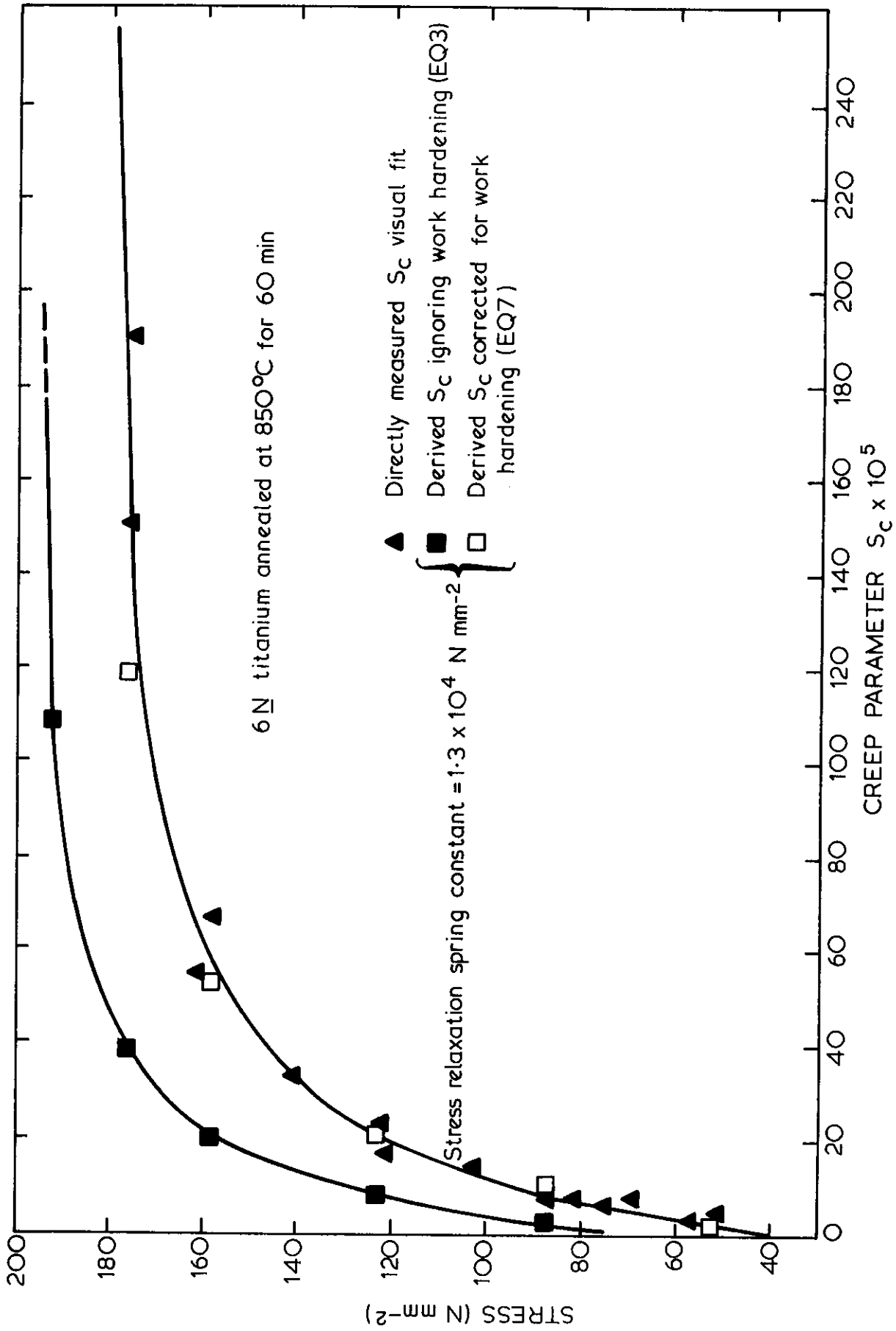
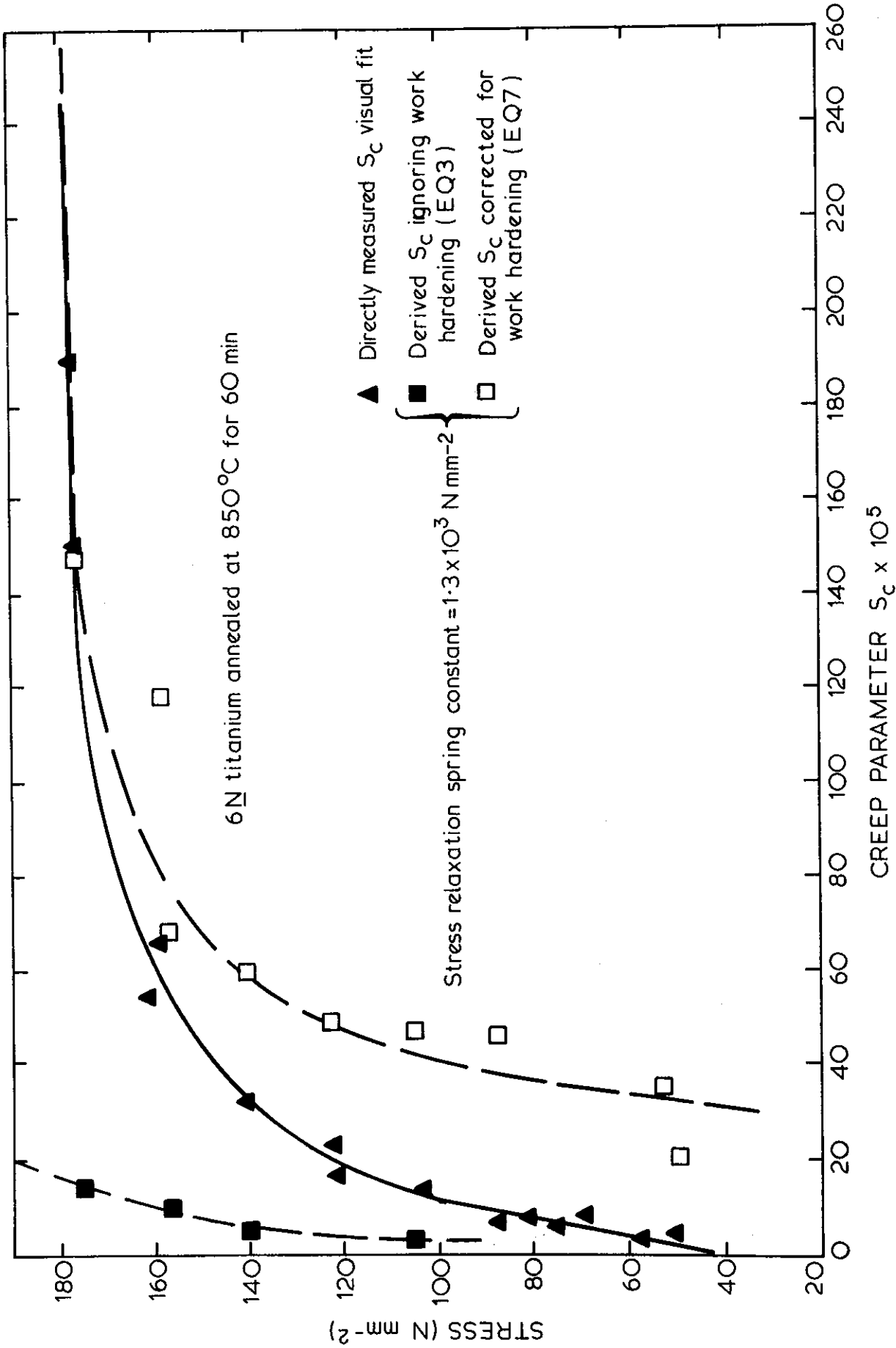


FIGURE 4. TITANIUM. DIRECTLY MEASURED AND DERIVED CREEP PARAMETERS  
 ( $\lambda = 1.3 \times 10^4 \text{ N mm}^{-2}$ ) VERSUS APPLIED STRESS



**FIGURE 5. TITANIUM. DIRECTLY MEASURED AND DERIVED CREEP PARAMETERS**  
 ( $\lambda = 1.3 \times 10^3 \text{ N mm}^{-2}$ ) VERSUS APPLIED STRESS

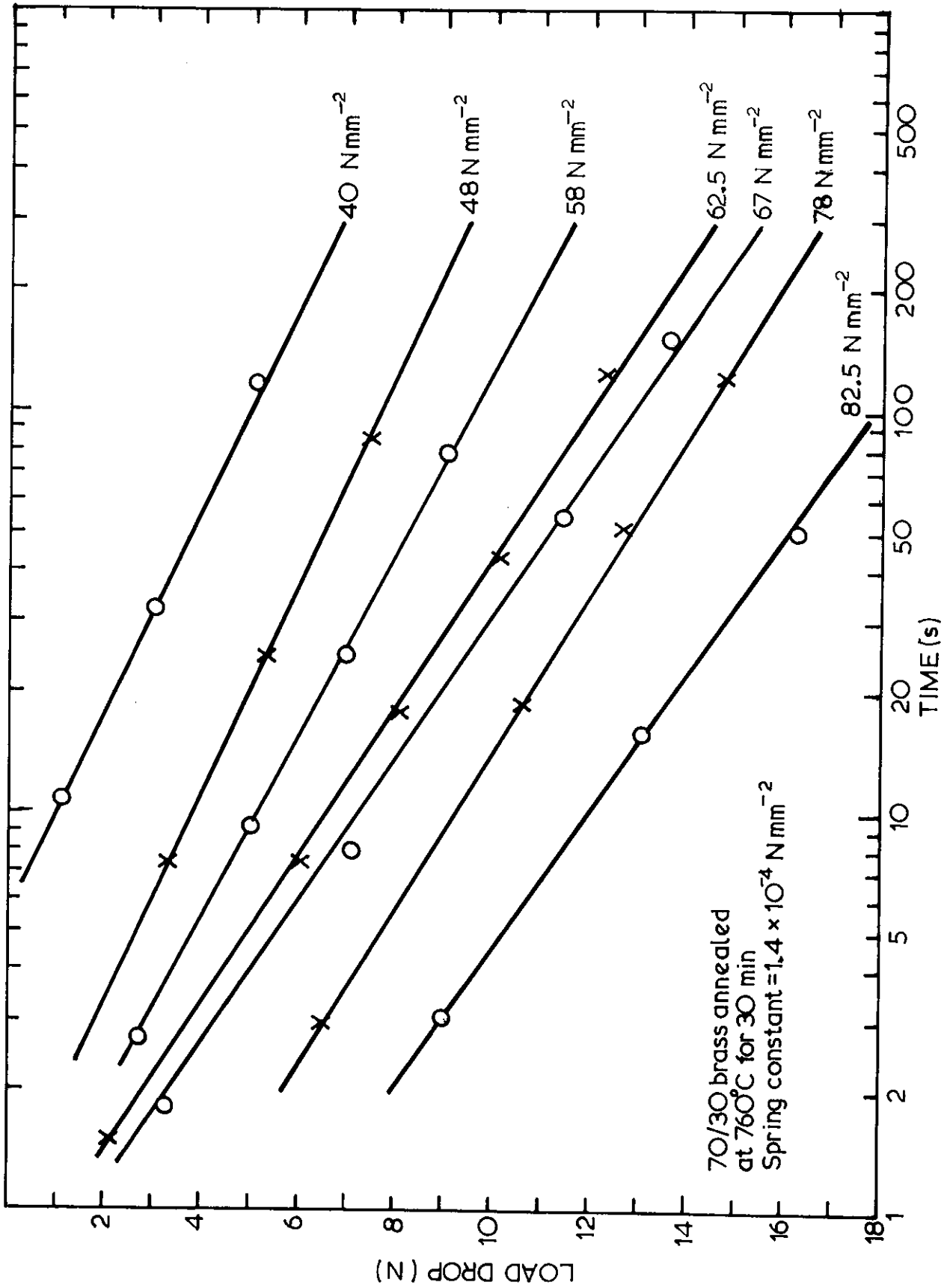


FIGURE 6. 70/30 BRASS. RELAXED LOAD VERSUS LOG TIME

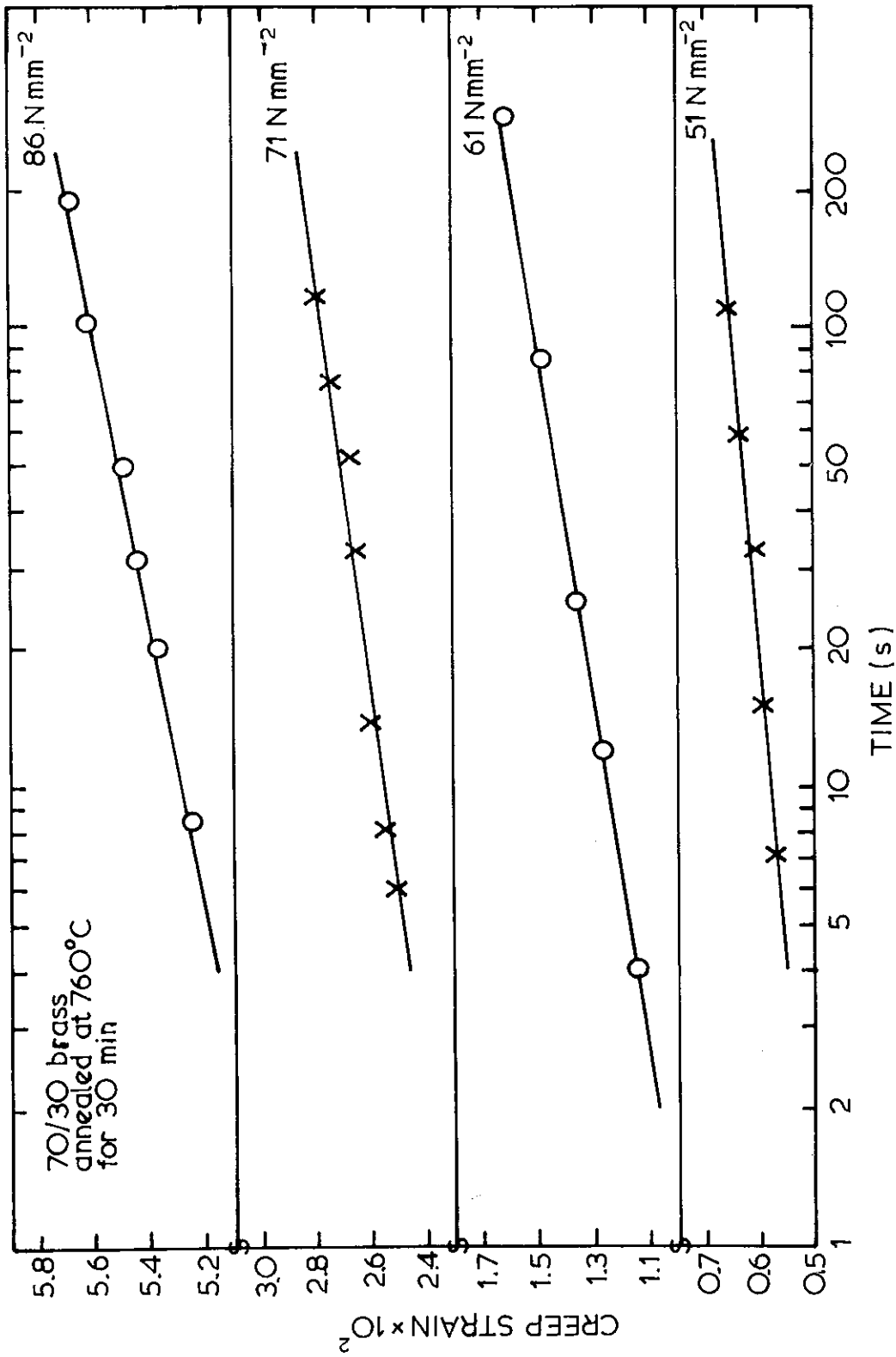


FIGURE 7. 70/30 BRASS. CREEP STRAIN VERSUS LOG TIME

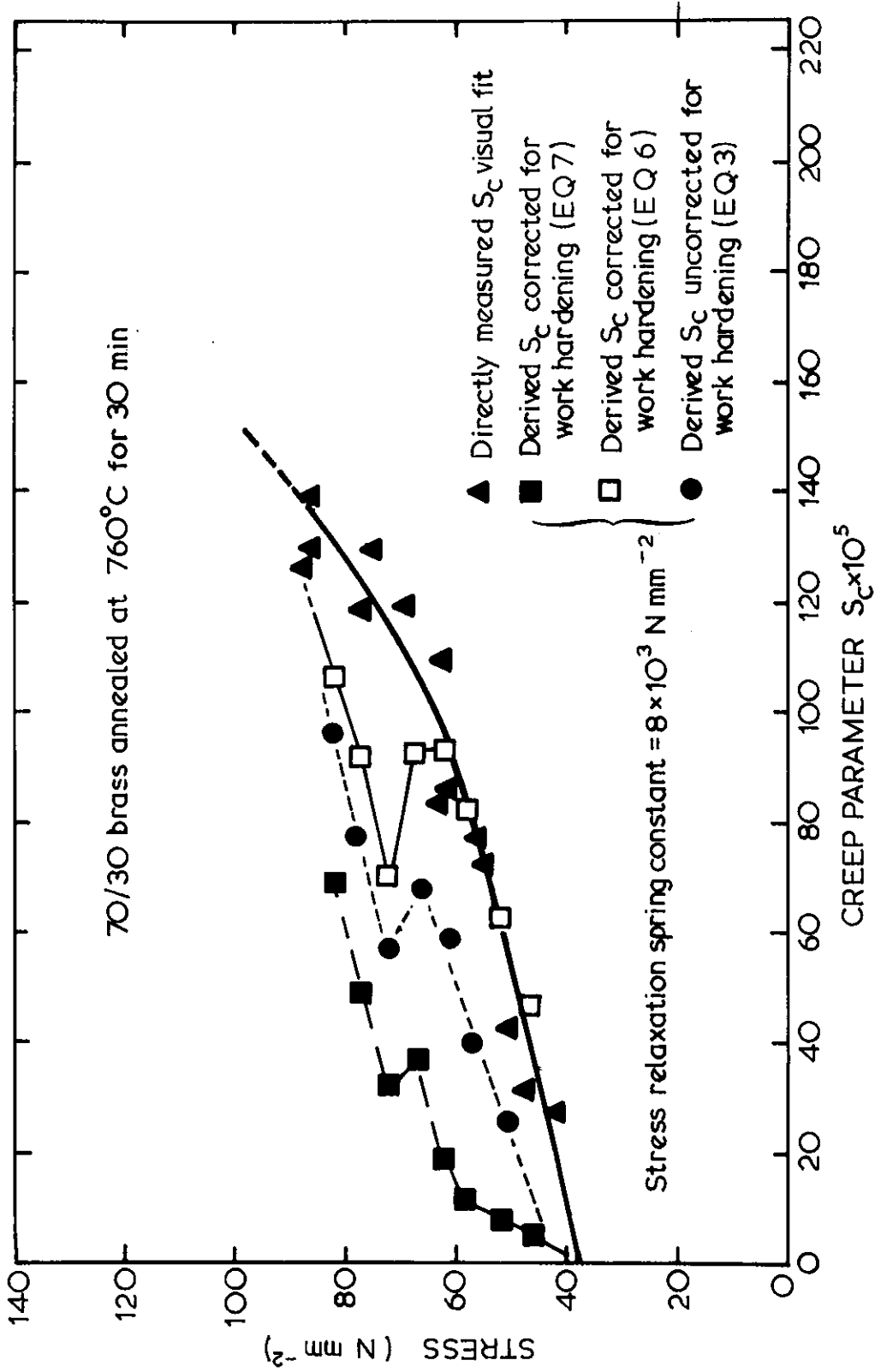


FIGURE 8. 70/30 BRASS. DIRECTLY MEASURED AND DERIVED CREEP PARAMETERS  
 ( $\lambda = 8 \times 10^3 \text{ N mm}^{-2}$ ) VERSUS APPLIED STRESS

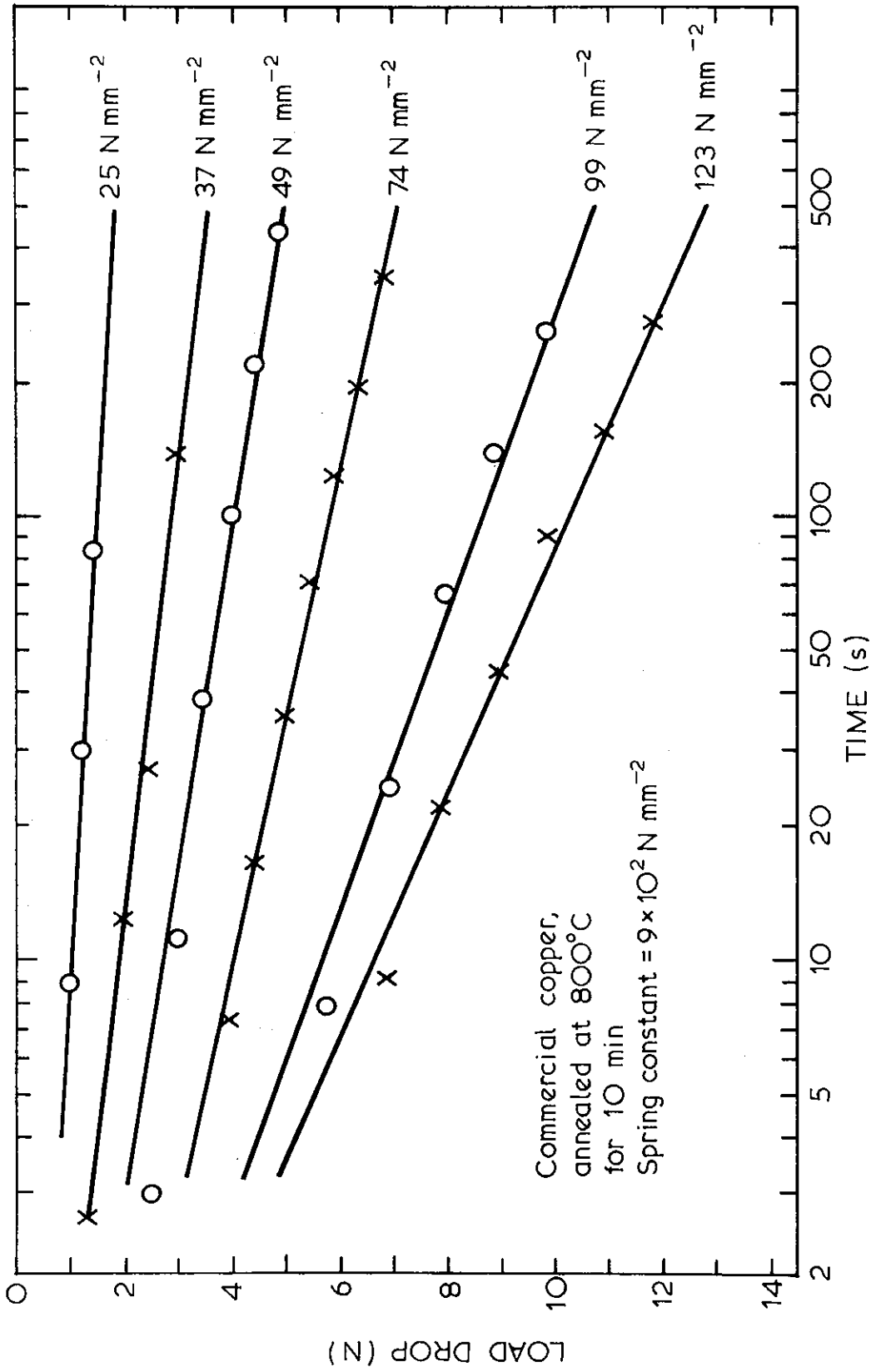


FIGURE 9. COPPER. RELAXED LOAD VERSUS LOG TIME (  $\lambda = 9 \times 10^2 \text{ N mm}^{-2}$  )

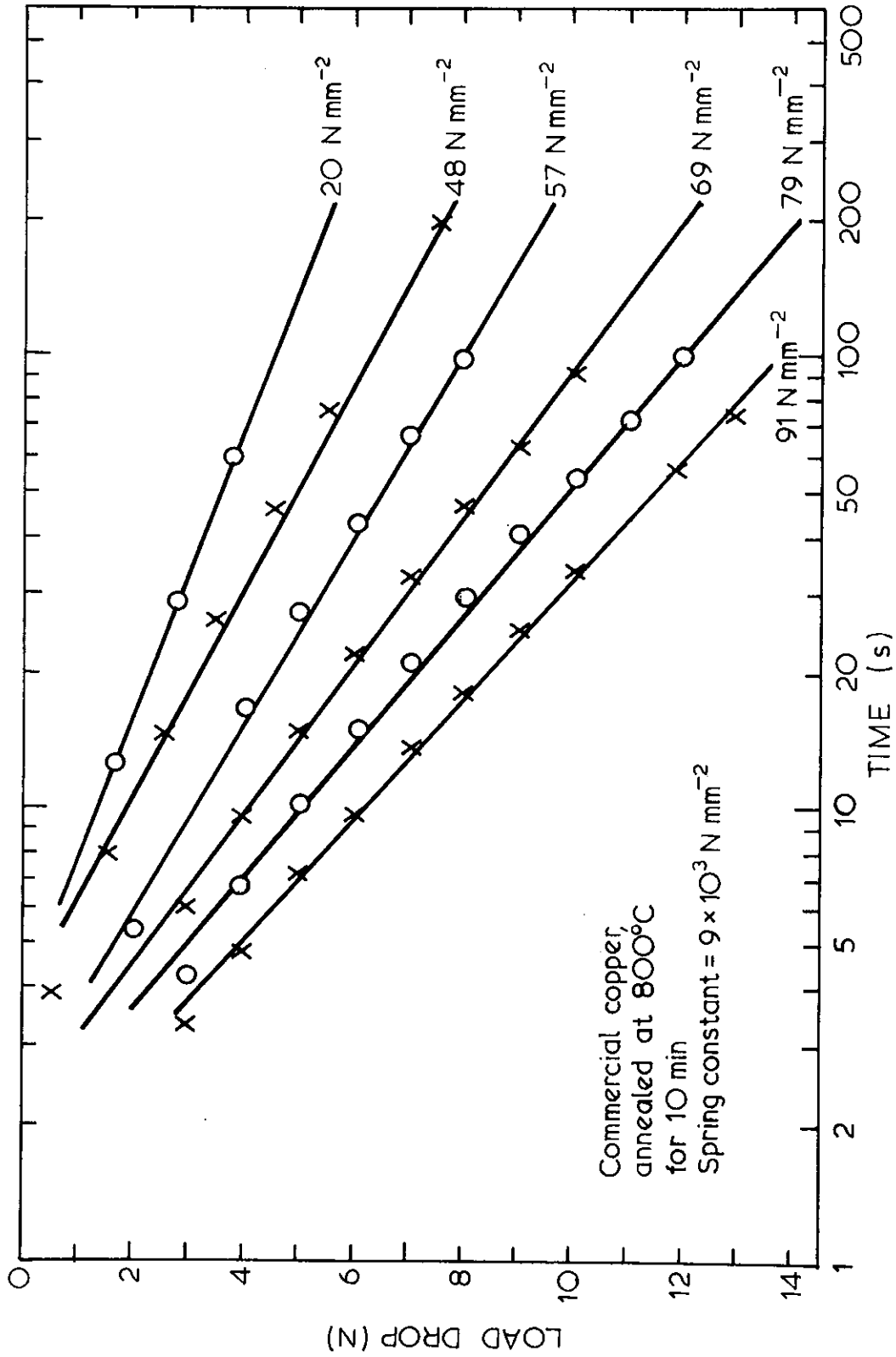


FIGURE 10. COPPER. RELAXED LOAD ( $\lambda = 9 \times 10^3 \text{ N mm}^{-2}$ ) VERSUS LOG TIME

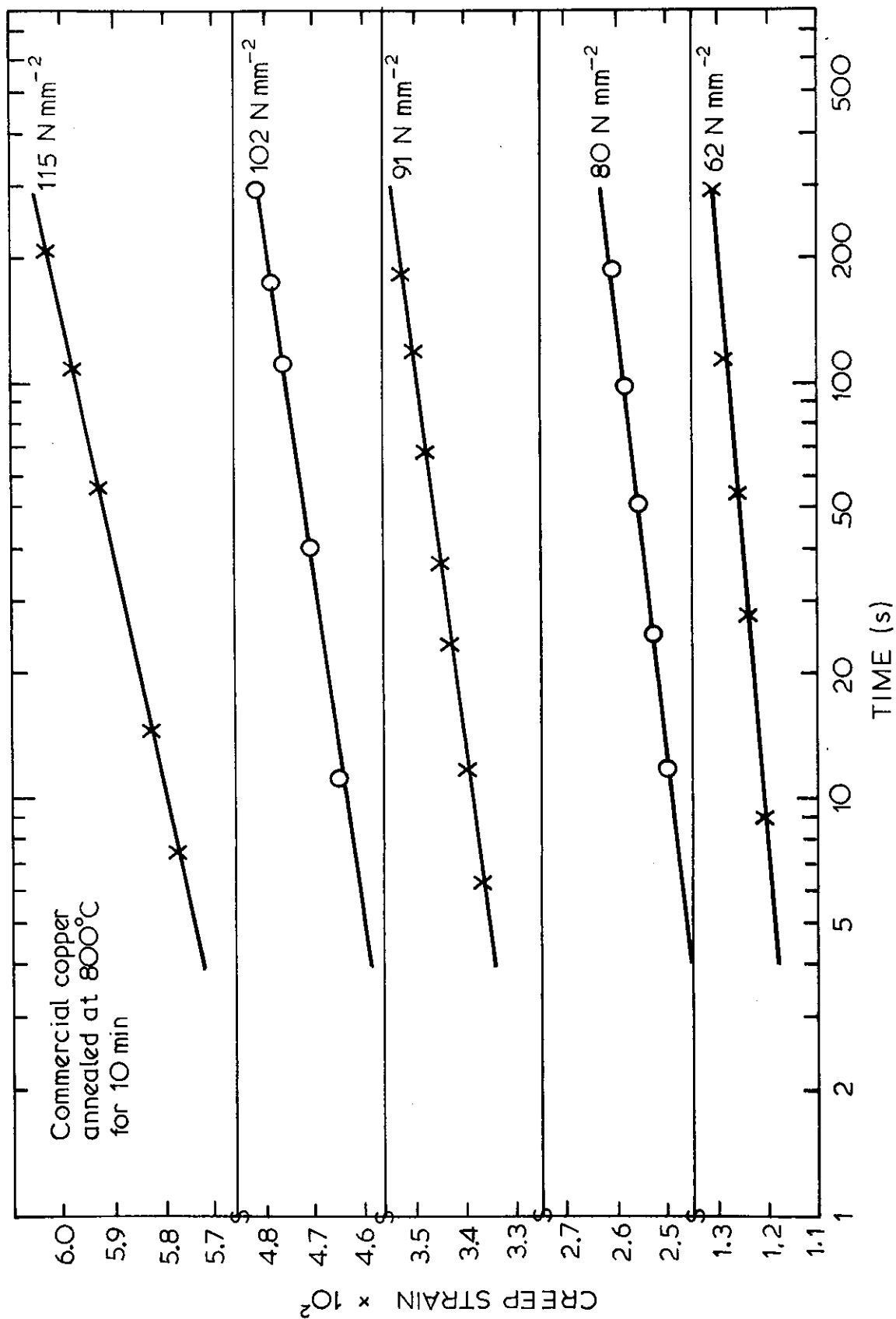


FIGURE 11. COPPER. CREEP STRAIN VERSUS LOG TIME

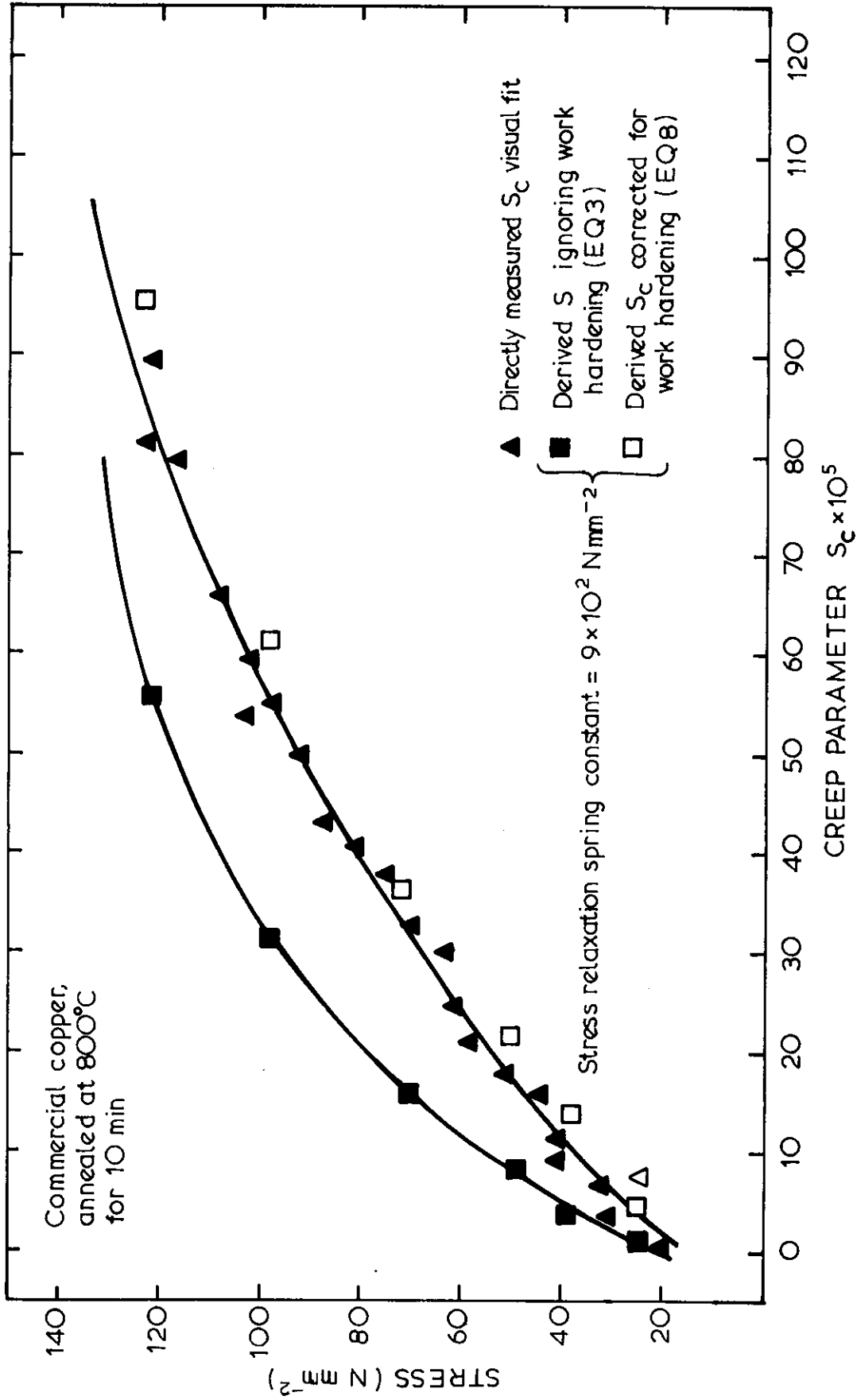


FIGURE 12. COPPER. DIRECTLY MEASURED AND DERIVED CREEP PARAMETERS  
(  $\lambda = 9 \times 10^2$  N mm<sup>-2</sup> ) VERSUS APPLIED STRESS

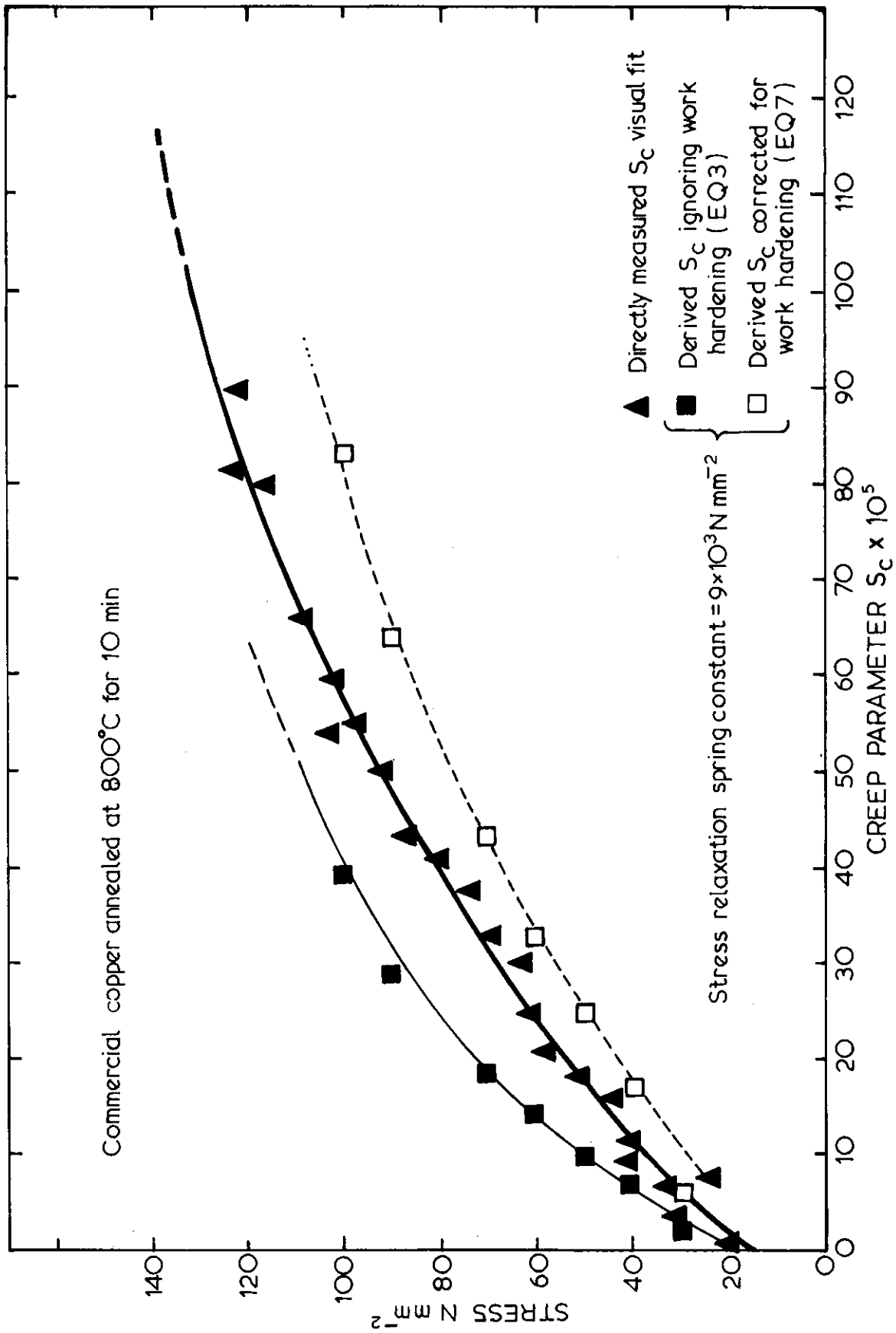


FIGURE 13. COPPER. DIRECTLY MEASURED AND DERIVED CREEP PARAMETERS  
 ( $\lambda = 9 \times 10^3 \text{ N mm}^{-2}$ ) VERSUS APPLIED STRESS

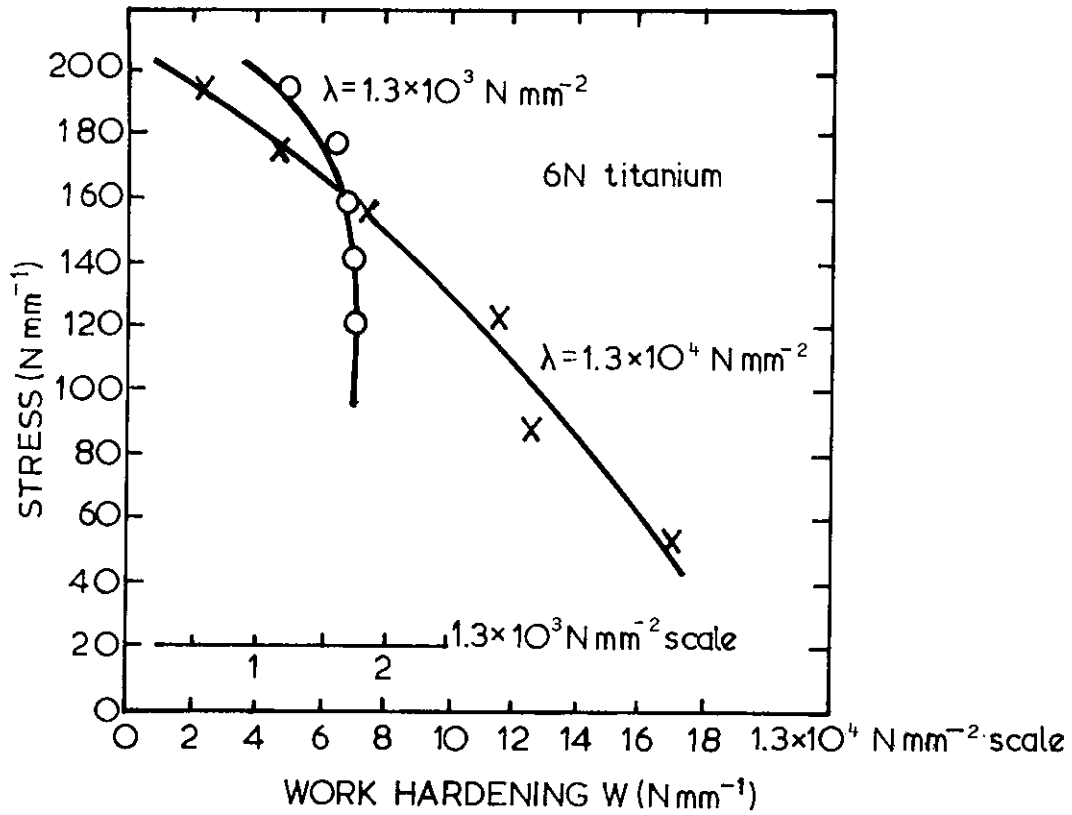


FIGURE 14. TITANIUM. WORK HARDENING SLOPE, W, VERSUS STRESS

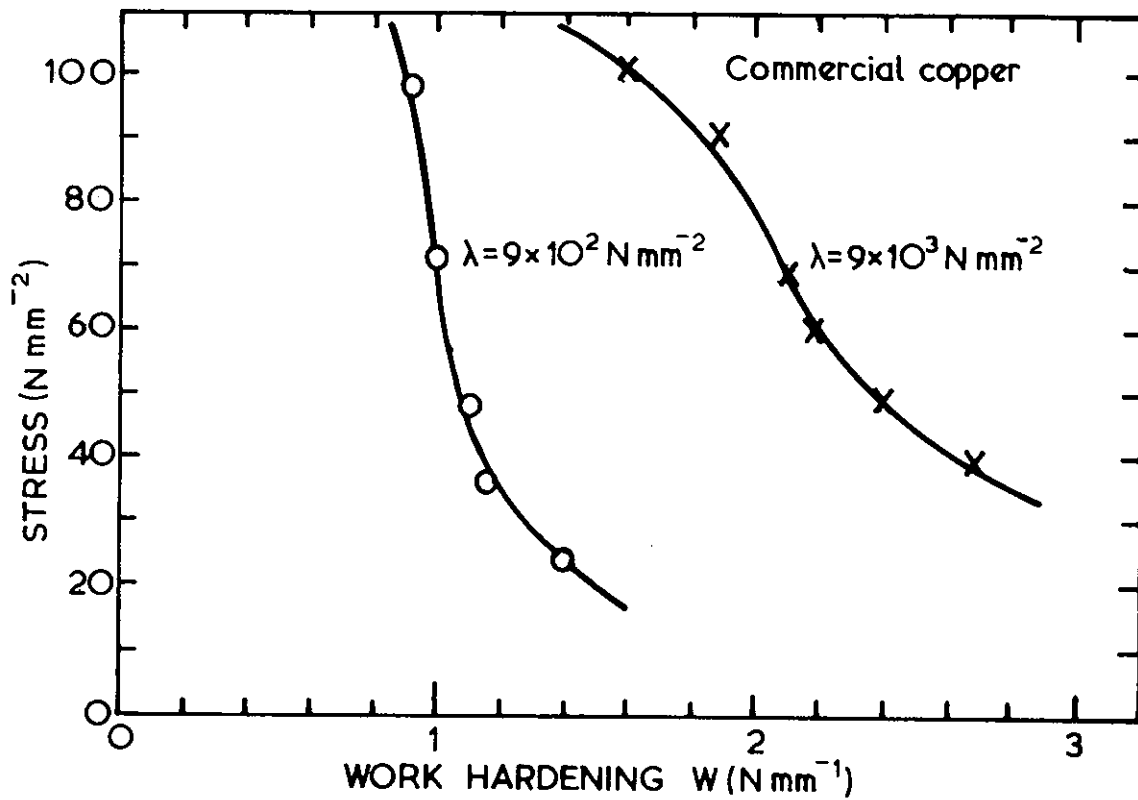


FIGURE 15. COPPER. WORK HARDENING SLOPE, W, VERSUS STRESS

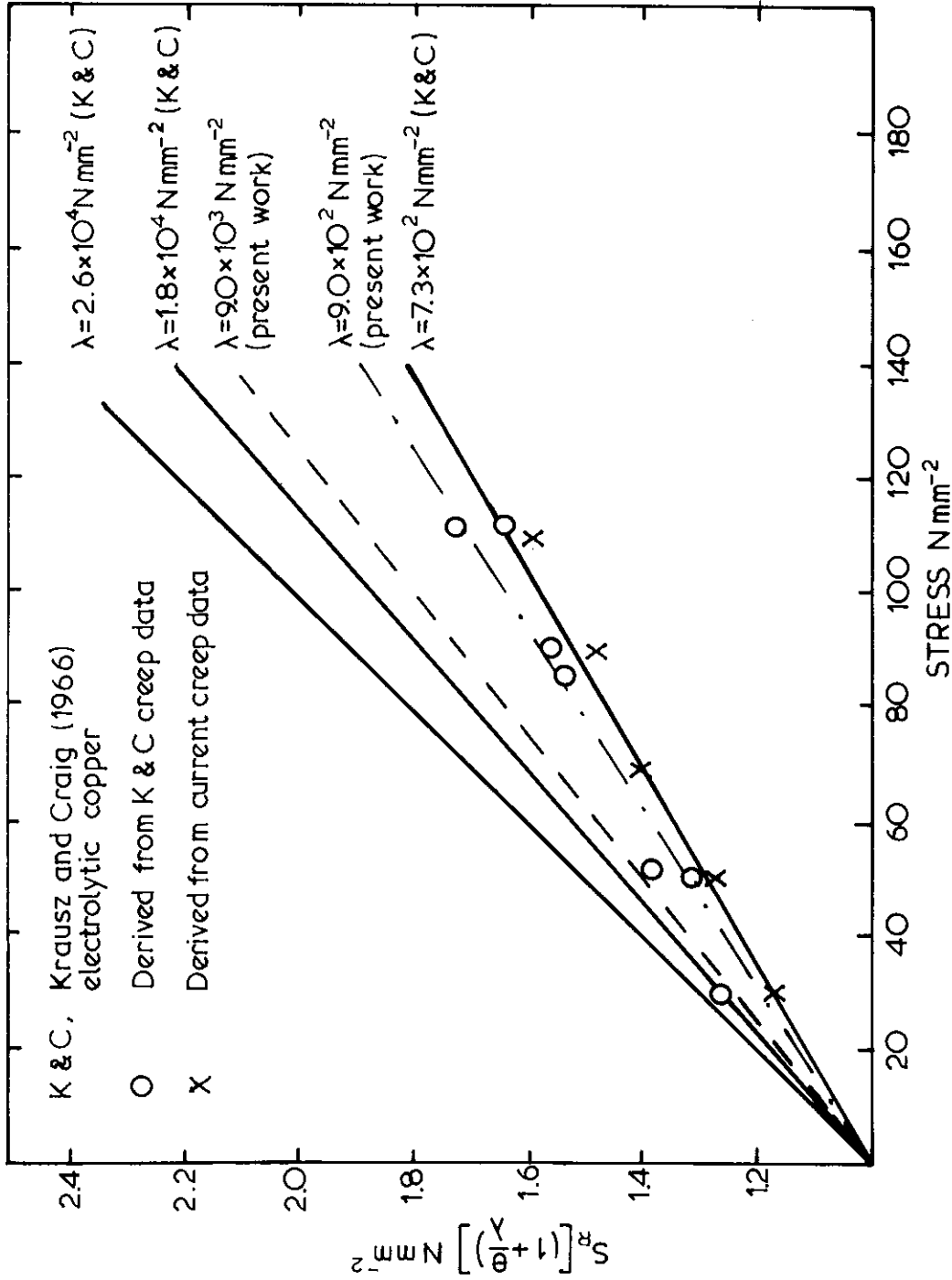


FIGURE 16. COPPER. STRESS RELAXATION PARAMETER, MEASURED AND DERIVED, VERSUS STRESS FOR VARIOUS SPRING CONSTANTS





$$= \frac{1}{\frac{X}{\Delta L} - \frac{Y}{\Delta L}} \times \frac{\dot{C}}{\dot{S}} \times \frac{\ell_0}{a_0}$$

$$\therefore \theta = \frac{M}{M-W} \times \frac{\dot{C}}{\dot{S}} \times \frac{\ell_0}{a_0}$$

This expresses  $\theta$  as it appears on the right hand side of Equation (6).

#### A2. Derivation of $(1 + \frac{\theta}{\lambda})$

$$\lambda = \frac{d\theta}{de_e}$$

over the load range  $\Delta L$ ,

$$d\sigma = \frac{\Delta L}{a_0}$$

and

$$de_e = Y \times \frac{\dot{S}}{\dot{C}} \times \frac{1}{\ell_0}$$

$$\therefore \lambda = \frac{\Delta L}{Y} \times \frac{\dot{C}}{\dot{S}} \times \frac{\ell_0}{a_0}$$

$$= M \times \frac{\dot{C}}{\dot{S}} \times \frac{\ell_0}{a_0}$$

Substituting for  $\theta$  and  $\lambda$ ,

$$\left(1 + \frac{\theta}{\lambda}\right) = 1 + \frac{\frac{MM}{M-W} \times \frac{\dot{C}}{\dot{S}} \times \frac{\ell_0}{a_0}}{M \times \frac{\dot{C}}{\dot{S}} \times \frac{\ell_0}{a_0}}$$

$$= 1 + \frac{W}{M-W}$$

$$\therefore \left(1 + \frac{\theta}{\lambda}\right) = \frac{M}{M-W}$$

This expresses  $(1 + \frac{\theta}{\lambda})$  as it appears on the left hand side of Equation (6).